



# Comparative Investigation of the Corrosion Protection Efficacy of *Spondias mombin* Leaf Extracts on AA2024 Alloy and Low Carbon Steel in Acidic Medium

Kalu D. Ogwo <sup>a\*</sup>, Lebe A. Nnanna <sup>b</sup>, Ahamefule C. Young <sup>c</sup>  
and Emea A. Eziyi <sup>d</sup>

<sup>a</sup> Department of Physics, College of Basic and Applied Science, Rhema University, Aba, Nigeria.

<sup>b</sup> Department of Physics, Michael Okpara University of Agriculture, Umudike, Nigeria.

<sup>c</sup> Department of Physics, Gregory University, Uturu, Abia State, Nigeria.

<sup>d</sup> Department of Physics, Clifford University, Owerrinta, Abia State, Nigeria.

## Authors' contributions

This work was carried out in collaboration among all authors. All authors read and approved the final manuscript.

## Article Information

DOI: 10.9734/PSIJ/2024/v28i3828

## Open Peer Review History:

This journal follows the Advanced Open Peer Review policy. Identity of the Reviewers, Editor(s) and additional Reviewers, peer review comments, different versions of the manuscript, comments of the editors, etc are available here: <https://www.sdiarticle5.com/review-history/114102>

Original Research Article

Received: 13/01/2024

Accepted: 17/03/2024

Published: 08/04/2024

## ABSTRACT

The anti-corrosive property of *Spondias mombin* (SM) leaves extract on low carbon steel (LCS) and aluminium alloy (AA2024) in 1M HCl solution was investigated using gravimetric and electrochemical methods. The results obtained from the weight loss experiment performed at various temperatures (30, 45, and 60 °C) show that the inhibition efficiency values decreased with temperature rise but increased as the inhibitor concentrations were increased. At 30 °C, optimum inhibition efficiency (IE) of 80.11% and 78.06% were obtained for LCS and AA2024 respectively. The potentiodynamic polarization (PDP) result reveal that an optimum IE values of 92.1% and

\*Corresponding author: E-mail: ogwodede@gmail.com, ogwo\_dede@rhemauniversity.edu.ng;

74.0% were respectively obtained for LCS and AA2024 while the electrochemical impedance spectroscopy (EIS) data show  $IE$  values of 91.5% and 74.5% for LCS and AA2024 respectively. In all cases, the values of inhibition efficiency obtained for LCS were greater than those obtained for AA2024. This implies that *SM* leaf extracts offers a better protective-layer on LCS surface compared to the AA2024 alloy in the acidic medium. The isotherm study reveal that Langmuir model best fitted the adsorption of the leaf extracts on LCS while Freundlich model best fitted the leaf extracts adsorption on AA2024 surface.

**Keywords:** AA2024 alloy; adsorption; protective-layer; isotherm.

## 1. INTRODUCTION

Aluminum alloy (AA2024) is light weight and belongs to the 2000 series which contains copper as its major alloying element. AA2024 alloy has applications in building and construction as well as in aerospace industries where material's weight and strength is of great essence [1]. Low carbon steel (LCS) has high mechanical strength and is relatively cheap when compared to the price of other alloys. These qualities make LCS economically useful in the construction of bridges, automobile body parts, oil pipes lines, heat exchanger, heat sink, and heat turbines. However, both aluminium and steel are susceptible to degradation when exposed to corrosive environment at elevated temperature [2]. Material deterioration of metals and alloys is mostly responsible for structural failures experienced in bridges, as well as in oil and gas, automotive, aerospace and naval industries [3,4,5,6]. In the petroleum and gas industries, over 50 % of the registered oil spills due to undetected cracks in steel pipelines are caused by corrosion [7]. In addition, failure of oil exploration equipment such as drilling rig can be attributed to corrosion which is as a result of exposure to high temperature acidic environment [8]. Over the years, inorganic and organic substances have been employed to check corrosion processes. However, organic compounds have been of major interest to researchers because they have been found to be biodegradable, eco-friendly, low in toxicity, and cost effective [9,10]. Organic substances that have been mostly used as corrosion inhibitor include; plant extracts [11,12], amino acids [13,14], and carbohydrates [15]. The ability of organic substances to retard corrosion of metals is related to the presence of tannins, alkaloids, flavonoids, and terpins [16,17]. These phytochemicals function by blocking the active sites of corrosion [18].

The aim of this work is to compare the corrosion mitigation effects and adsorption mechanism of

*Spondias mombin* leaves extracts on aluminium alloy (AA2024) and low carbon steel (LCS) in acidic medium. The reported Phytochemical screening of *Spondias mombin* leaves shows that the plant contains; 3.82% of tannins, 7.6% of saponins, 6 % of alkaloids, 3 % of flavonoids, and 1% phenols [19]. The use of *Spondias mombin* leaves extract as a corrosion inhibitor has been investigated by several researchers [20,21,22,23]. However, these works were mostly limited to the anti-corrosive performance of *Spondias mombin* leaves extract on mild steel in acidic medium. The corrosion inhibitory effects of *Spondias mombin* leaves extract could possibly be influenced by the choice of metal or alloy used. This observation encouraged the comparative investigation of the corrosion inhibition effects of the leaf extracts on the selected metals in acidic medium (1 M HCl) using gravimetric analysis, potentiodynamic polarization (PDP), and electrochemical impedance spectroscopy (EIS) techniques.

## 2. MATERIALS AND METHODS

### 2.1 Leaves Extracts Preparation

The *Spondias mombin* leaves were obtained from *New Market*, Aba, Abia State, Nigeria. The leaves were air-dried and crushed to powder using grinding machine. 0.015 kg mass of the ground leaves were loaded into a 24 x 80 mm cellulose extraction thimble and was refluxed severally in 15 mL ethanol boiling at a temperature of 78 °C. A dark purple coloured solution containing mixture of ethanol and the leaves extract was obtained after four hours. The solution was heated again to evaporate ethanol, leaving behind a semi-solid substance. The extracts concentration ranging from 0.1 - 0.5 g/l were weighed and dissolved in 1 M HCl.

### 2.2 Corrodent Preparation

The HCl used has purity of 37% and density of 1.2 g/cm<sup>3</sup>. Acid volume of 82.2 cm<sup>3</sup> was diluted in

917.8 cm<sup>3</sup> of distilled water, using the serial dilution method to obtain a 1.0 M Hydrochloric acid medium.

### 2.3 Metals Preparation

The aluminium alloy (AA2024) and low carbon steel (LCS) used for this experiment were obtained from Federal University of Petroleum Resources, Effurun, Nigeria and Kaiser Aluminum, Sokane, respectively. The elemental composition of the low carbon steel and AA2024 is shown in Tables 1 and 2 respectively. The metal samples were cut to a dimension of 1.0 cm x 1.0 cm coupons and were polished with emery paper of different grades. The coupons were degreased in ethanol, washed with distilled water, air dried and stored in moisture free environment.

### 2.4 Weight loss Measurement

The pre-weighed metal coupons of AA2024 and low carbon steel were suspended with the aid of hangers and immersed in 150 ml of 1 M HCl blank solution and in 150 ml of 1 M HCl solution containing various concentrations of *SM* leaves extracts at 30 °C temperature. The immersed coupons were retrieved progressively at 2 hours intervals for 10 hours, and were washed, air dried, and re-weighed. The weight loss was obtained by taking the difference in weight of the specimen before and after immersion. The experiments were performed in triplicates for good reproducibility and were repeated at elevated temperatures of 45, and 60 °C.

### 2.5 Electrochemical Measurements

The potentiodynamic polarization (PDP) and electrochemical impedance spectroscopy (EIS) measurements were performed at room temperature. The PDP measurements were performed using the conventional three cells system; the working electrode (1cm x 1cm AA2024 coupon), the reference electrode (saturated calomel electrode), and the counter electrode ( 1 cm x 1cm platinum plate). For the PDP measurements, the working electrodes were immersed in a test solution (1 M HCl) containing no inhibitor and solution which contains various inhibitor concentration for half an hour. The dynamic polarization curves were obtained at a 1 mV/s scan rate within a potential range of -0.25 V to +0.25 V.

The EIS measurements were performed over a frequency domain range of 10 Hz to 100kHz at

room temperature using amplitude of 5 mV peak to peak ac signal at the open circuit potential and at air atmosphere. The EIS data was analyzed using EC301 potentiostat attached with SRS Lab software.

## 3. RESULTS AND DISCUSSION

### 3.1 Weight loss Measurement

Values obtained from the weight loss experiment were used calculate the corrosion rates (C.R) of the metals, inhibition efficiencies (%) of the inhibitor, and surface coverage ( $\theta$ ) using equations 1, 2 and 3 respectively.

$$C.R = \frac{k\Delta w}{\rho At} \quad (1)$$

where;

K = constant for unit conversion with value of 87.6,  $\Delta$   
W = weight loss of the coupon in g,  
 $\rho$  = density of coupon in g/cm<sup>3</sup>,  
A = Area of coupon in cm<sup>2</sup>,  
t = exposure time in hours

$$I(\%) = \frac{p_0 - p_1}{p_0} \times 100 \% \quad (2)$$

Where;  $p_1$  and  $p_0$  are respectively the corrosion rate in the presence and absence of the inhibitor.

$$\theta = \frac{I(\%)}{100} \quad (3)$$

The plots of the corrosion rates of LCS and AA2024 against inhibitor concentration at various temperatures after 6 hours of exposure are respectively shown in Fig. 1a and 1b.

The plots show that for the uninhibited environment, LCS deteriorated at a higher rate reaching value of 15.02 mm/yr, compared to 13.294 mm/yr obtained for AA2024. The plots also indicate a significant decrease in the corrosion rates of both metals in the inhibited environment compared to the blank. The corrosion rates of both metals were found to increase with temperature rise but decreased with increasing concentration of the inhibitor. The reduction in corrosion rates as inhibitor concentration is increased implies an adsorption of the adsorbate on the metal's surface resulting to the formation of protective film [24]. The plots of the inhibition efficiency versus inhibitor concentration (Fig. 2a and 2b) show an increase

in efficiency of the inhibitor as the concentration is increased but a decline inefficiency as temperature rises. This is suggestive of physical adsorption of the inhibitor molecules on the metals surface [25]. An optimum inhibition

efficiency of 80.11% and 78.06% were obtained for LCS and AA2024 respectively. This implies that *Spondias mombin* leaves extract has a slightly higher inhibition efficacy for LCS in the acidic medium compared to the AA2024 alloy.

**Table 1. Elemental composition of low carbon steel**

Element	C	Mn	Si	P	S	Cu	Pb	Ve	Mo	Fe
Actual(wt%)	0.05	1.13	0.05	0.91	0.85	0.09	0.15	0.13	0.08	96.56

**Table 2. Elemental composition of low carbon steel**

Element	Si	Fe	Cu	Mn	Mg	Cr	Zn	Ti	V	Al
Actual (wt%)	0.08	0.19	4.61	0.55	1.3	0.01	0.11	0.06	0.05	93.13

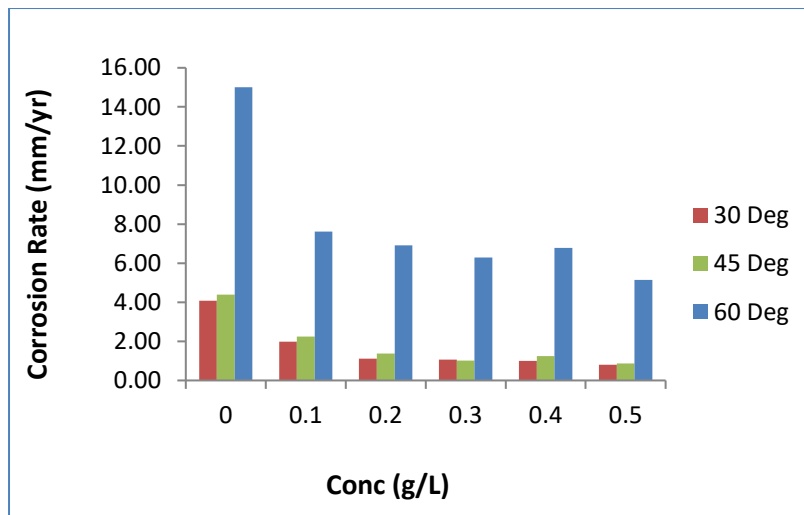


**Fig. 1a. Corrosion rate of LCS versus concentration at various temperatures**

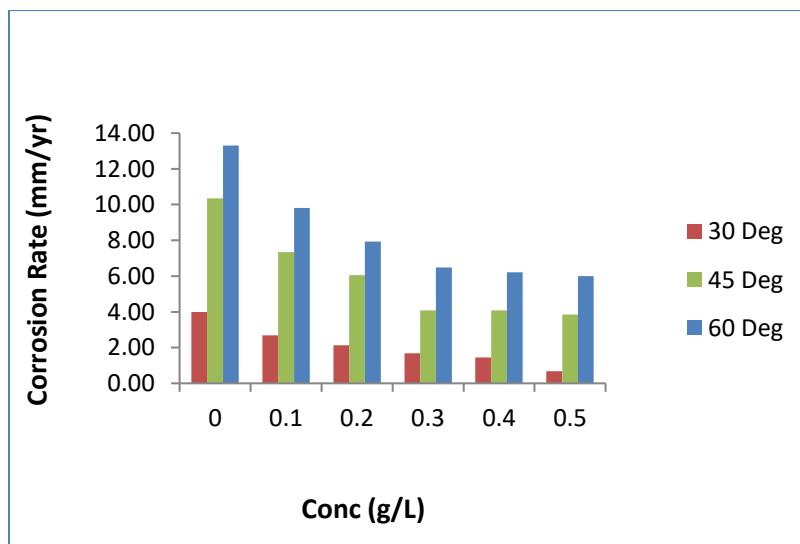


**Fig. 1b. Corrosion rate of AA2024 versus concentration at various temperatures**

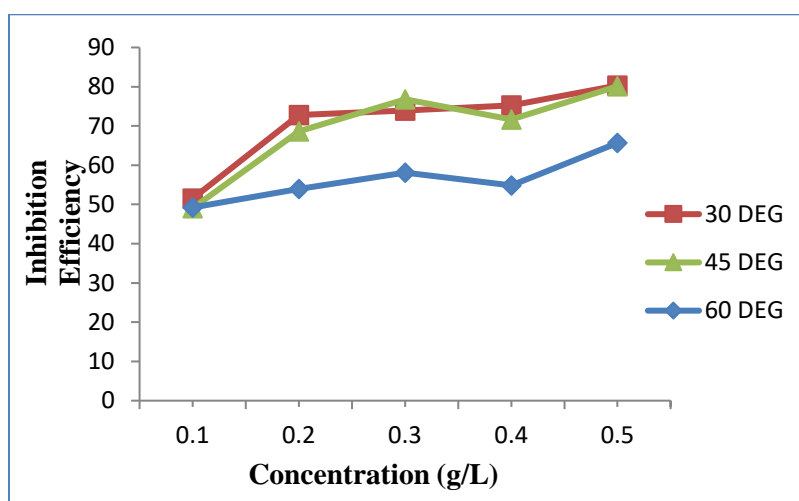


Fig. 2a. Inhibition efficiency of Spondias M. extracts on LCS in 1 M HCl at various temp

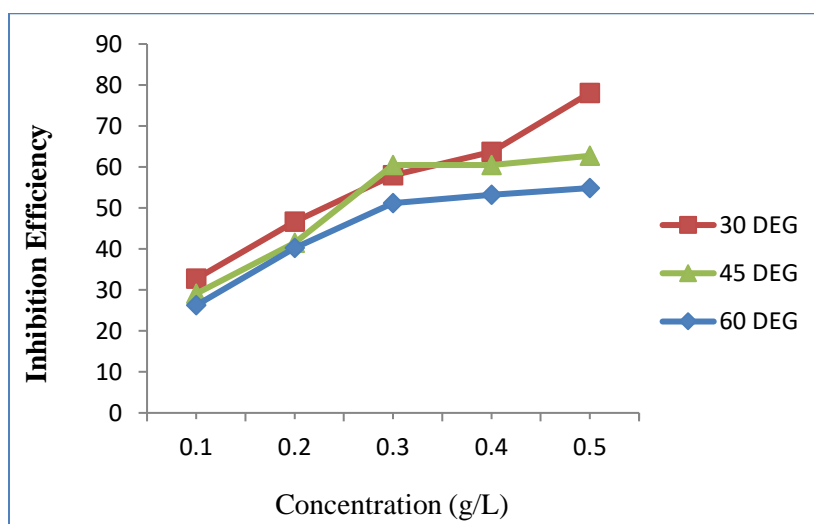


Fig. 2b. Inhibition efficiency of Spondias M. extracts on AA2024 in 1 M HCl at various temp

### 3.2 Potentiodynamic Polarization Result

The potentiodynamic polarization curves (Tafel plot) of LCS and AA2024 exposed to 1M of HCl environment in the presence and absence of SM leaf extracts are respectively shown in Fig. 3a and 3b. The plots indicate a decrease in corrosion current density ( $i_{corr}$ ) as the concentration of the inhibitor increased. This implies that the anodic dissolution of the metals and cathodic reduction of hydrogen ions were inhibited; suggesting a reduction of the active surface area and the formation of a protective layer of the adsorbate molecules over the surface of the metals [26]. Table 3 show the values of the PDP parameters obtained. Table 3 show that the corrosion potential ( $E_{corr}$ ) tend toward negative values for all concentration and

the maximum displacement shift values were less than 85mV which indicate that *Spondias mombin* leaf extract behave as mixed inhibitor [27]. The inhibition efficiency was calculated using the equation,

$$IE = \frac{i_{corr}^0 - i_{corr}^{in}}{i_{corr}^0} \times \frac{100}{1} \quad (4)$$

where  $i_{corr}^0$  is the corrosion current density for the blank and  $i_{corr}^{in}$  is the corrosion current density for the inhibited system. An optimum inhibition efficiency value of 92.1% and 74.0% were respectively obtained for LCS and AA2024 which is in close conformity with values obtained for the weight loss experiment. This indicate that the leaf extract offers a slightly higher protective coverage to mild steel compared to AA2024 in 1 M HCl.

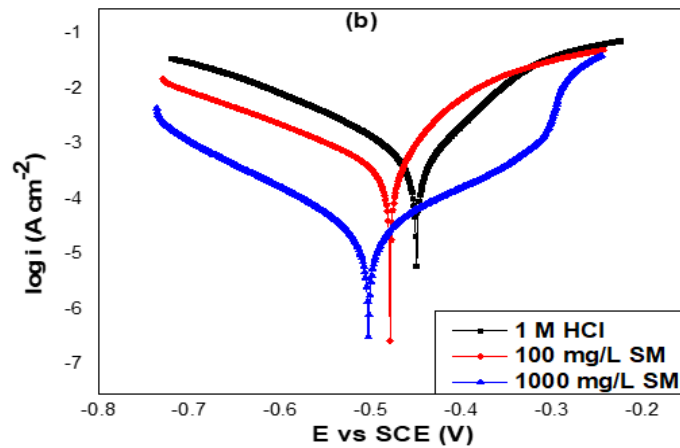


Fig. 3a. PDP plot of LCS in 1 M HCl in the absence and presence of SM

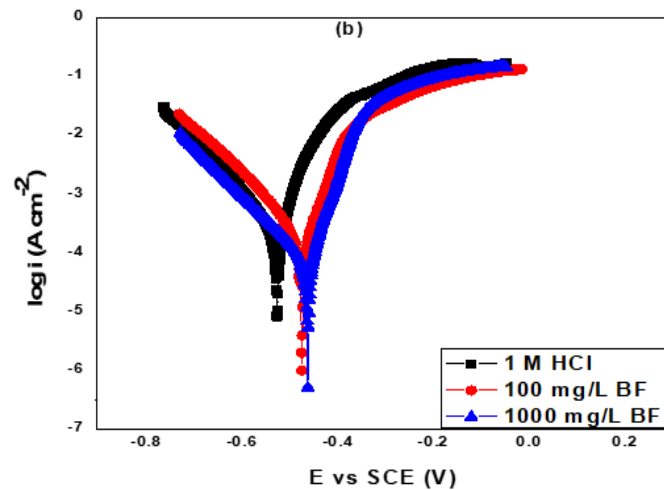


Fig. 3b. PDP plot of AA2024 in 1 M HCl in the absence and presence of SM

Table 3. Potentiodynamic polarization parameters for LCS and AA2024 in 1 M HCl in the Absence and Presence of *Spondias mombin* extracts

Metal	C(mg/L)	$E_{corr}$ (mV/SCE)	$I_{corr}$ ( $\mu$ A/cm <sup>2</sup> )	% I.E
Low	Blank	-436.4	157.8	-
Carbon	100	-488.2	20.4	87.1
Steel	1000	-502.3	12.5	92.1
AA2024	Blank	-558.4	154.8	-
Alloy	100	-445.5	63.5	59.0
	1000	-487.7	40.2	74.0

### 3.3 Electrochemical Spectroscopy

The Nyquist plots of LCS and AA2024 exposed to 1M of HCl environment in the presence and absence of *Spondias mombin* extracts are respectively shown in Fig. 4a and 4b. The plots show a unit capacitive-like, depressed semi-circular loop extending over the frequency range. The trend of the Nyquist plots reveals that the

### Impedance

higher the concentration of the inhibitor, the more the increase in radius which suggest a charge transfer process between the adsorbate and adsorbent [28] and also confirm that the leaf extract as an adsorption inhibitor for both metals in 1M solution of HCl. The loops were characterized by imperfect semi-circles which can be attributed to the inhomogeneities and roughness of the metals' surface [29].

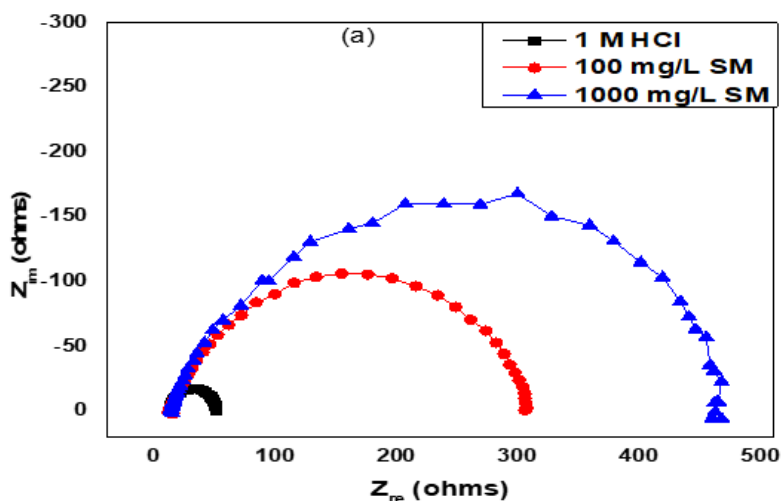


Fig. 4a. Nyquist plot of LCS in 1 M HCl environment in the absence and presence of SM

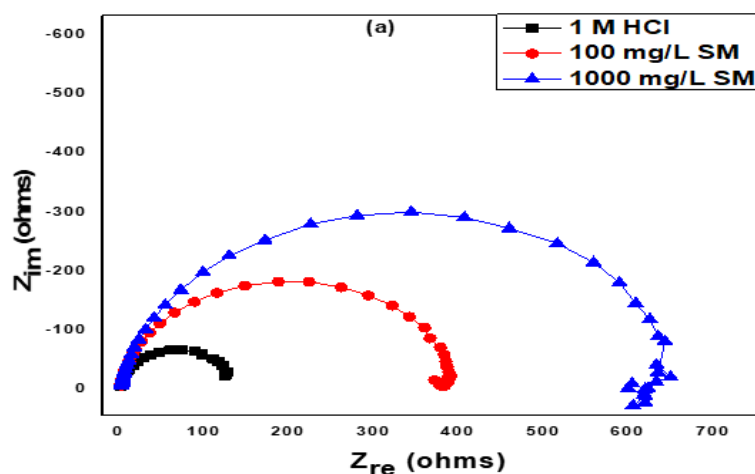


Fig. 4b. Nyquist plot of AA2024 in 1 M HCl environment in the absence and presence of SM

The impedance parameters were obtained using EIS equivalent circuit model which consist of solution resistance  $R_s$ , charge transfer resistance  $R_{CT}$  and pure capacitor of double layer  $C_{dl}$  as shown Fig. 5. The charge transfer resistances  $R_{CT}$  represents the real impedance value and depends on the low frequency data while the solution resistance  $R_s$  depends on the high frequency data. The EIS inhibition efficiency can be obtained using values of the charge transfer resistance as shown in equation 5;

$$I\% = \frac{R_{CT} - R_{CT}^0}{R_{CT}} \quad (5)$$

Where;  $R_{CT}$  is the charge transfer resistance in the presence of inhibitor and  $R_{CT}^0$  is the charge transfer resistance in the absence of inhibitor.

The values of the electrochemical impedance parameters obtained are recorded in Table 4. The table shows an increase in  $R_{CT}$  values as the inhibitor concentration is increased which could be attributed to the formation of protective layer at the metal-solution interface. The table also shows that for LCS, inhibition efficiency values of 86.7% and 91.5% were respectively obtained at 100mg/L and 1000 mg/L concentration while for AA2024, an inhibition efficiency of 57.5% and 74.5% were respectively obtained at 100 mg/L and 1000 mg/L concentration. This implies that *Spondias mombin* leaves extract offers a better anti-corrosives layer on LCS surface compared to AA2024 alloy in the acidic medium. This corroborates with the results obtained for the weight loss and potentiodynamic experiments.

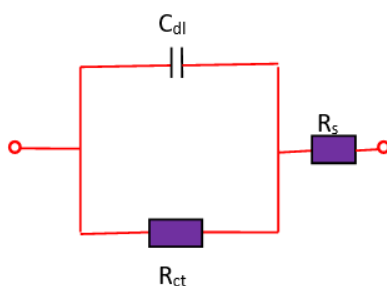


Fig. 5. EIS Equivalent circuit

Table 4. Electrochemical Impedance Parameters for LCS and AA2024 in 1 M HCl in the Absence and Presence of *Spondias mombin* extracts

Metal/alloy	C(mg/L)	n	$R_{ct}(\Omega\text{-cm}^2)$	$R_{Li}(\Omega\text{-cm}^2)$	% I.E
Low	Blank	0.89	39.7	-	-
Carbon	100	0.88	298.6	-	86.7
Steel	1000	0.89	467.8	-	91.5
AA2024	Blank	0.89	156.7	-	-
Alloy	100	0.89	368.7	309.6	57.5
	1000	0.89	614.5	619.2	74.5

Table 5. Adsorption isotherm parameter of *Spondias M.* leaves extract on low carbon steel in 1 M HCl environment at various temperatures

T (K)	Langmuir			Temkin				Freundlich			
	$R^2$	$K_{ads}$	$\Delta G_{ads}$ (kJ/mol)	$R^2$	a	$K_{ads}$	$\Delta G_{ads}$ (kJ/mol)	$R^2$	N	$K_{ads}$	$\Delta G_{ads}$ (kJ/mol)
303	0.994	14.08	-16.781	0.876	0.082	1.16	-10.501	0.855	3.921	0.98	-10.082
318	0.983	12.34	-17.263	0.865	0.088	1.17	-11.054	0.855	3.533	1.00	-10.618
333	0.968	13.69	-18.365	0.715	0.040	1.05	-11.270	0.744	6.944	0.68	10.056

Table 6. Adsorption isotherm parameter of *Spondias M.* leaves extract on AA2024 in 1 M HCl environment at various temperatures

T (K)	Langmuir			Temkin				Freundlich			
	$R^2$	$K_{ads}$	$\Delta G_{ads}$ (kJ/mol)	$R^2$	a	$K_{ads}$	$\Delta G_{ads}$ (kJ/mol)	$R^2$	n	$K_{ads}$	$\Delta G_{ads}$ (kJ/mol)
303	0.953	4.11	-13.681	0.958	0.132	1.272	-10.725	0.991	1.926	1.075	-10.301
318	0.956	4.34	-14.504	0.931	0.113	1.229	-11.164	0.936	1.960	0.969	-10.536
333	0.985	4.34	-15.188	0.967	0.092	1.162	-11.535	0.947	2.114	0.824	-10.585

### 3.4 Isotherm Studies

In isotherm studies, the linearity of a graph and good correlation coefficient ( $R^2$ ) may be interpreted to suggest that the experimental data for the studied inhibitor obey a particular adsorption isotherm. The adsorption behaviour of *Spondias mombin* leaves extract on low carbon steel (LCS) and AA2024 alloy was investigated by fitting data obtained from the weight loss temperature variation measurements into different adsorption isotherms. The Langmuir, Temkin, and Freundlich isotherms model are

represented by equations; 6, 7 and 8 respectively.

$$\frac{C}{\theta} = \frac{1}{K_{ads}} + C \tag{6}$$

$$\theta = \frac{1}{f} \ln k_{ads} + \frac{1}{f} \ln C \tag{7}$$

$$\log_e \theta = \log_e k + \log_e C \tag{8}$$

Where  $\theta$  is the degree of surface coverage, C is inhibitor's concentration, f determines the adsorbent-adsorbate interaction, n describes the



adsorbate type ( $0 < n < 1$ ) and  $K_{ads}$  is the adsorption equilibrium constant used in calculating the Gibb's free energy of adsorption ( $\Delta G_{ads}$ ).

$$\Delta G_{ads} = -RT \ln(55.5K_{ads}) \quad (9)$$

where R is the gas constant with value of 8.314 kJ/mol and T is the temperature in Kelvin and 55.5 is the concentration of water in the solution in mol/L. Adsorption data obtained from the isotherm studies are presented in Tables 4 and 5. Table 4 shows maximum  $R^2$  values of 0.994 for Langmuir, 0.876 for Temkin, and 0.855 for Freundlich isotherms at 30 °C temperature, while Table 5 shows maximum  $R^2$  values of 0.953 for Langmuir, 0.958 for Temkin, and 0.991 for Freundlich isotherms 30 °C temperature. The  $R^2$  results reveal the Langmuir model best fitted the adsorption of the inhibitor on LCS while Freundlich isotherm best fitted the inhibitor adsorption on AA2024 surface. The values of the equilibrium adsorption constant  $K_{ads}$  were found to decrease with temperature rise which indicate decline in adsorption of the adsorbate on the metal's surface. The negative values of  $\Delta G_{ads}$  indicate that the adsorption process of the leaves extract was spontaneous [30]. More so, the calculated  $\Delta G_{ads}$  values shown in Tables 4 and 5 were all greater than -20 kJ/mol which suggest that the adsorption process of the leaves extract follows physisorption mechanism. The values adsorbent-adsorbate interaction term "a" were all positive and less than unity. This implies the existence of a lateral attractive force between the BF and SM molecule and the adsorption layer [31].

#### 4. CONCLUSION

Anti-corrosive effects of *Spondias mombin* leaves extract on aluminium alloy (AA2024) and low carbon steel (LCS) was investigated using weight loss and electrochemical methods. From the result obtained, the following conclusions were made;

1. The leaves extract of *Spondias mombin* inhibited the corrosion of AA 2024 alloy and low carbon steel in 1 M HCL solution by physical adsorption.
2. The inhibition efficiencies were found to increase with increase in concentration of inhibitor but decreased with temperature rise.
3. In all cases, the values of inhibition efficiency obtained for LCS were greater

than those obtained for AA2024. This implies that SM leaves extract offers a better anti-corrosives layer on LCS surface compared to the AA2024 alloy in the acidic medium.

4. The free energy ( $\Delta G^{\circ}_{ads}$ ) adsorption ( $\Delta G^{\circ}_{ads}$ ) has negative values. This indicates that the adsorption of the *Spondias mombin* extract on the surface of both metals follows a spontaneous process.

#### COMPETING INTERESTS

Authors have declared that no competing interests exist.

#### REFERENCES

1. Pekok MA, Setchi R, Ryan M, Han Q, Gu D. Effect of process parameters on the microstructure and mechanical properties of AA2024 fabricated using laser melting", International Journal of advanced manufacturing technology. 2021;112:175-192.
2. Hawraa K, Adman A, Amjed A. The effect of temperature and inhibitor on corrosion of carbon steel in acid solution under static study, International journal of applied engineering research. 2018; 13(6): 3638-3647.
3. Chengli Song, Yuanpeng Li, Fan Wu, Jinheng Luo, Lifeng Li, Guanshan Li. "Failure analysis of crack and leakages of a crude oil pipeline under CO<sub>2</sub>-steam flooding", Processes. 2023;11:5. Available: <https://doi.org/10.3390/pr1105167>
4. Antonia Menga, Terje Kanstad, Daniel Cantero, Lise Bathen, Karla Hornbostel, Anja Klausen. Corrosion induced damages and failures of posttensioned bridges: A literature review, Structural Concrete. 2022; 24(1):84-99.
5. Mladena Lukovic, Branko Savija, Guang Ye, Eric Schlangen, Klaas van Breugel. Failure Modes in concrete systems due to ongoing corrosion, Advances in Materials Science and Engineering; 2017. Article ID 9649187, 14 pages, 2017 Available: <https://doi.org/10.1155/2017/9649187>
6. Magdalena Czaban. Aircraft corrosion – Review of corrosion processes and its effects in selected cases. Fatigue of Aircraft Structures. 2017;5-20. Available: <https://doi.org/10.2478/fas-2018-0001>

7. Obike Anthony, Uwakwe Kelechi, Abraham E, Ikeuba Alexander and Emori Winifred. "Review of the losses and devastation caused by corrosion in the Nigerian oil industry for over 30 years, International Journal of corrosion and scale inhibition. 2020;9(1):74-91.
8. Sedmak A, Radzeya Zaidi, Borivoje Vujcic. Corrosion effects on structural integrity and life of oil rig drill pipes, Hemijska Industrija. 2022;76(3):167-177.
9. Sethuraman MG, Raja PB. Corrosion inhibition of mild steel by Daturametel in acidic medium, Pig. Resin Tech. 2008; 34(6):327-331.
10. Brycki BE, Kowalczyk IH, Szulc A, Kaczerewska O, Pakiet M. Organic Corrosion Inhibitors. In (Ed.), Corrosion inhibitors, Principle and recent Applications Intech; 2017.  
Open://doi.org/10.5772/intech.72943
11. Inesemet AA, Okon UA, Mfon AJ. inhibition of mild steel corrosion in acid medium by rind extract of Telfairia occidentalis, Asian Journal of Applied Chemistry Research. 2018;1(3):1-10,
12. Ekanem UF, Umoren SA, Udousoro SA, Udoh AP. Inhibition of Mild Steel Corrosion in HCL using Pineapple Leaves Extract, Journ. of Mat. Sci. 2010;45:5558-5566.
13. Yeganeh M., Khosravi-Bigdelio, Alevi R. Corrosion inhibition of L-methionine amino acid as a green corrosion inhibitor for stainless steel in H<sub>2</sub> SO<sub>4</sub> solution, Journal of Materials engineering and performance. 2020;29:3983-3994.
14. El Ibrahim B, Bazzi L, El Issami S. Amino acids and their derivatives as corrosion inhibitors for metals and alloys, Arabian Journal of chemistry. 2017;13(1):740-771.
15. Rbaa M, Fardioui M, Chandrabhan V, Ashraf S, Abousalem M, Galai EE. Ebenso T, Guedira B. Lakhrissi I. Warad A. Zarrouk. 8-Hydroxyquinoline based chitosan derived carbohydrate polymer as biodegradable and sustainable acid corrosion inhibitor for mild steel: Experimental and computational analyses, International journal of biological macromolecules. 2020;155:645-655.
16. Zakerio Ali, Bahmani Elnaz, and Aghdam Alireza. Plant extracts as sustainable and green corrosion inhibitors for protection of ferrous metals in corrosive media: A mini review, Corrosion Communications. 2022; 5: 25-38.
17. Ngobiri N, Obi C. Corrosion inhibition behaviour of eneantia chlorantha extract on pipeline steel corrosion in acidic system, Journal of applied science and environmental management. 2020;24 (4): 707-712.
18. Begum AS, Vahith RM, Abdelgawad A, Awwad EM, Khan M. Spilanthes acmella leaves extract for corrosion on inhibition in acid medium. Coatings. 2022;11:106.
19. Njoku PC, Akumefula MI. "Phytochemical and nutrient evaluation of spondias mombine. Pakistan Journal of nutrition. 2007;6(6):613-615.
20. Obi-Egbedi NO, Obot IB, Umoren SA. Spondias mombin L. as a green corrosion inhibitor for aluminium in sulphuric acid: Correlation between inhibitive effect and electronic properties of extracts major constituents using density functional theory, Arabian Journal of Chemistry, vol. 2012;5(3):361- 373.
21. Adama KK, Onyeachu BI. Inhibitory action of Spondias mombin leaves extracts on corrosion of mild steel in 1 M HCl. Nigerian Journal of Technological Development. 2023;20(1).
22. Magu TO, Ugi BU. Inhibition, Adsorption and thermodynamic Investigation of Iron Corrosion by Green Inhibitors in Acidic Medium" Int. Journal of Science and Technoledge. 2017;5: 56-64.
23. Kalu D. Ogwo, Lebe A. Nnanna, Ugomma C. Onyeije AD. Asiegbu, Electrochemical Investigation of the Anti-corrosive Effect of Spondias mombin Leaves Extract on the Corrosion of Aluminium Alloy (AA2024) and Mild Steel in 0.5 M NaCl, Chemical Science International Journal. 2023;32 (3):44-51.
24. Iroha NB, Madueke NA, Mkpennie V, Ogunyemi BT, Lebe AN, Sangeeta Singh Ekemini D. Akpan Eno E. Ebenso. Experimental, adsorption, quantum chemical and molecular dy-namics simulation studies on the corrosion inhibition performance of Vincamine on J55 steel in acidic medium Journal of Molecular Structure; 2020.  
Available:https://doi.org/10.1016/j.molstruc.2020.129533
25. Gomez sanches G, Olivares Xometl O, Arellanes Lozada P, Likhanova NV, Lijanova IV, Arrriola Morales J. Temperature effect on the corrosion inhibition of carbon steel by polymericionic

- liquids in acidic medium. Intern. Journal of molecular science. 2003; 24:6291.
26. Saeed Ur Rahman, Abraham Atta Ogwu. Corrosion and Mott-Schottky probe of chromium nitride coatings exposed to saline solution for engineering and biomedical applications Advances in Medical and Surgical Engineering. 2020; 239–265.
27. Araceli E, Manuel A, Guillermo E, Francisco J. Manuel P, Leticia L, Deyanira Á, Diego P. Carbohydrates as Corrosion Inhibitors of API 5L X70 Steel Immersed in Acid Medium, Int. J. Electrochem. Sci. 2019;14:9206–9220.
28. Solomon MM, Umoren SA. Electrochemical and gravimetric measurements of inhibition of aluminium corrosion by poly (metahcrylic acid) in H<sub>2</sub>SO<sub>4</sub> solution and synergistic effect of iodide ions, Measurements. 2015;76:104-116.
29. El Ibrahim B, Jmiai A, El Mouaden K. Theoretical evaluation of some α-amino acids for corrosion inhibition of copper in acidic medium. DFT calculations. Monte Carlo simulations and QSPR studies, Journal of king Saud university-science. 2020;32(1):163-171.
30. Abubakar I, Feyisayo VA, Joshua OM, Ifeoma VJ, Peter AO. Corrosion Inhibition of Mild Steel in 1M Hydrochloric Acid using Haematostaphis barteri Leaves Extract 2nd International Conference on Sustainable Materials Processing and Manufacturing. 2019;35:1279–1285.
31. Ogwo KD, Osuwa JC, Udoinyang IE, Nnanna LA. Corrosion inhibition of mild steel and aluminium in 1M HCL Acid by leaves extract of ficus symorus, Physical Science International Journal. 2017;14 (3):1-10.

© Copyright (2024): Author(s). The licensee is the journal publisher. This is an Open Access article distributed under the terms of the Creative Commons Attribution License (<http://creativecommons.org/licenses/by/4.0>), which permits unrestricted use, distribution, and reproduction in any medium, provided the original work is properly cited.

*Peer-review history:*

*The peer review history for this paper can be accessed here:*

*<https://www.sdiarticle5.com/review-history/114102>*